

Quantum routing of single photons with whispering-gallery resonators

Jin-Song Huang*,¹ Jia-Hao Zhang,¹ and L. F. Wei^{†2,3}

¹*School of Information Engineering, Jiangxi University of Science and Technology, Ganzhou 341000, China*

²*Information Quantum Technology Laboratory, School of Information Science and Technology, Southwest Jiaotong University, Chengdu 610031, China*

³*State Key Laboratory of Optoelectronic Materials and Technologies, School of Physics, Sun Yat-Sen University Guangzhou 510275, China*

Quantum routing of single photons in a system with two waveguides coupled to two whispering-gallery resonators (WGRs) are investigated theoretically. With a real-space full quantum theory, photonic scattering amplitudes along four ports of the waveguide network are analytically obtained. It is shown that, by adjusting the geometric and physical parameters of the two-WGR configuration, the quantum routing properties of single photons along the present waveguide network can be controlled effectively. For example, the routing capability from input waveguide to another one can significantly exceed 0.5 near the resonance point of scattering spectra, which can be achieved with only one resonator. By properly designing the distance between two WGRs and the waveguide-WGR coupling strengths, the transfer rate between the waveguides can also reach certain sufficiently high values even in the non-resonance regime. Moreover, Fano-like resonances in the scattering spectra are designable. The proposed system may provide a potential application in controlling single-photon quantum routing as a novel router.

PACS numbers: 42.50.Ex, 03.65.Nk, 42.79.Gn, 42.60.Da

I. INTRODUCTION

In the realization of various quantum network [1], quantum nodes, coherently connecting different quantum channels, are particularly important ingredients. Quantum routers [2, 3], as one kind of node devices, are usually utilized to control the path of the quantum signals. Recent development of the single-photon transport technique [4–8] provides an ideal tool to design various desired quantum networks, wherein photonic waveguides are served as the quantum channels for propagating singles and the quantum routers are utilized to control the single photons in the channels. Indeed, many theoretical [9–15] and experimental [16, 17] works have demonstrated how to design various quantum routers for controlling the photonic transports in quantum networks.

Typically, Zhou and Lu et al [9, 10] proposed a routing approach to control the photonic propagations in the X-shaped coupled-resonator waveguide. Also, single-photon routing scheme for the usual optical waveguide with multiple ports has been proposed by Yan et al [11]. However, the expectable routing probabilities in these configurations are limited no more than 0.5 by a single two-level atom or a single bosonic mode, and thus restrict more practical applications. To overcome partially such a difficulty, we proposed an alternative scheme [18] to implement various designable routing probabilities for arbitrarily selected ports, by using a series of atomic mirrors. Still, the routing capability of the single photon controlled by the atomic mirrors is strongly influenced by their unavoidable dissipations. Therefore, looking for the robust quantum router to implement the single-photon routing with high probability in multiple waveguide network is still a challenge and thus of considerable interest.

It is well-known that the whispering-gallery resonator (WGR), which supports two bosonic modes, is one of the attractive optical devices. Particularly, due to its very low loss rate achieved experimentally and the special construction of its cyclic modes, the WGR possesses the potential advantage for many quantum optical applications. Actually, with the WGRs, numerous single-photon devices such as quantum switches [19–22], photonic transistors [23, 24], quantum routing networks [1, 25], entangled photon-pair generators [26], and optomechanical devices [27–31], etc., have been demonstrated. Continuously, in this paper we design a double-WRG quantum router to control the single-photon transport in a double-waveguide quantum network.

By adopting a full quantum theory on single-photon transports in real space [8], we investigate how the single-photon can be controlled in the waveguide network by using the scatterings by a pair of WRGs with the inter-resonator distance and the resonator-waveguide coupling strength being designable. The amplitudes of single-photon being scattered into the four ports of the network are obtained analytically. Then, by numerical method we discuss how to design the relevant geometric and physical parameters to implement the desired quantum routings of the single photons. It is shown that the quantum routing property of the single photons into these four ports can be controlled really by adjusting backscattering strength between the two degenerate mode of WGR. In contrast to previous schemes [9–11] with a maximum transfer rate 0.5, the probability of single photons routed from input channel to another can significantly exceed 0.5 near resonance even for a single resonator, due to the special cyclic mode of the resonator to redirect the photons to another waveguide. High routing capability can also be realized by varying the distance of two WGRs and the coupling between waveguides and WGRs in the nonresonance regime. Additionally, we find that the Fano-like resonances, due to the quantum interference, are also be designed for its potential applications.

The paper is organized as follows. Sec. II shows our theo-

*jshuangjs@126.com

†weilianfu@gmail.com

retical model and its exact solution. Accordingly in Sec. III, by numerical method we investigate how to adjust double-WGR router parameters to implement high routing capabilities of single photons, and discuss the controls of the Fano-like resonances in the present configuration. Our conclusions are summarized finally in Sec. IV.

II. THEORETICAL MODE

The considered waveguide network is illustrated schematically in Fig. 1, wherein two WGRs coupled to two waveguides are separated with a distance d . The waveguides are utilized as the quantum channels, and each of the WGRs supports two degenerate modes, i.e., the clockwise- and counterclockwise ones. The black lines and red lines denote the counterclockwise and clockwise propagations of the incident photon, respectively. R_m and T_m ($m = a, b$) represent the reflection and transmission amplitudes in the m th-waveguide of the single photons, which is incident from the left of the waveguide- a and routed by the WGRs into the four ports of the network.

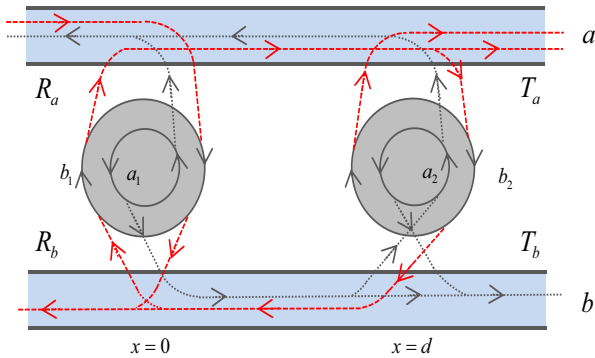


FIG. 1: (Color online) Schematic routings of single photons in two photonic waveguides (labeled as a and b , respectively), controlled by two WGRs with respective degenerate modes, a_n and b_n ($n = 1, 2$). Here, the red and the black lines represent the clockwise and counterclockwise propagations, respectively. R_a , R_b and T_a , T_b are the reflection and transmission amplitudes of the photons, respectively.

Suppose that the photonic dispersions in the waveguide [8] are linear. Then the effective real-space Hamiltonian for the

present network can be written as

$$\begin{aligned}
 H/\hbar = & \int dx \left\{ \sum_{m=a,b} [-iv_g \frac{\partial}{\partial x} C_{Rm}^\dagger(x) C_{Rm}(x) \right. \\
 & + iv_g \frac{\partial}{\partial x} C_{Lm}^\dagger(x) C_{Lm}(x)] \\
 & + V_{1a} \delta(x) [C_{Ra}^\dagger(x) b_1 + C_{La}^\dagger(x) a_1 + H.c.] \\
 & + V_{1b} \delta(x) [C_{Rb}^\dagger(x) a_1 + C_{Lb}^\dagger(x) b_1 + H.c.] \\
 & + V_{2a} \delta(x-d) [C_{Ra}^\dagger(x) b_2 + C_{La}^\dagger(x) a_2 + H.c.] \\
 & + V_{2b} \delta(x-d) [C_{Rb}^\dagger(x) a_2 + C_{Lb}^\dagger(x) b_2 + H.c.] \left. \right\} \\
 & + \sum_{n=1,2}^{m=a,b} [(\omega_{cn} - \frac{i\gamma_{cn}}{2}) m_n^\dagger m_n + h_n (a_n^\dagger b_n + b_n^\dagger a_n)].
 \end{aligned} \tag{1}$$

Here, $C_{Rm}^\dagger(x)/C_{Lm}^\dagger(x)$ denotes the creation operator of the right/left-moving photon at x in the waveguide- m . v_g is the group velocity of the photons and V_{nm} ($n = 1, 2; m = a, b$ throughout the paper) the coupling strength between the n th WGR and the waveguide- m . $\delta(x)/\delta(x-d)$ indicates that the interaction between the waveguide and the WGR occurs at $x = 0/d$. Also, a_n^\dagger (a_n) is the bosonic creation (annihilation) operator for the counterclockwise mode of the n th WGR, while b_n^\dagger (b_n) for the clockwise mode of the n th WGR with the eigenfrequency ω_{cn} . γ_{cn} is the dissipation rates of the n th WGR mode, and h_n is the backscattering strength between the clockwise mode and counterclockwise mode, respectively.

Assume that the photon is incident from the left in the waveguide- a with the energy $E_k = v_g k$. The scattering eigenstates of the Hamiltonian (1) are given by

$$\begin{aligned}
 |\psi\rangle = & \sum_{m=a,b} \int dx [\phi_{Rm}(x) C_{Rm}^\dagger(x) \\
 & + \phi_{Lm}(x) C_{Lm}^\dagger(x)] |\emptyset_a, \emptyset_b, 0, 0, 0, 0\rangle \\
 & + \xi_1 |\emptyset_a, \emptyset_b, 1, 0, 0, 0\rangle + \xi_2 |\emptyset_a, \emptyset_b, 0, 1, 0, 0\rangle \\
 & + \xi_3 |\emptyset_a, \emptyset_b, 0, 0, 1, 0\rangle + \xi_4 |\emptyset_a, \emptyset_b, 0, 0, 0, 1\rangle
 \end{aligned} \tag{2}$$

where $\phi_{Rm/Lm}$ is the single photon wave function in the right/left of the waveguide- m . $|\emptyset_a, \emptyset_b, 0, 0, 0, 0\rangle$ describes the vacuum states of the waveguides and the WGRs. ξ_1 and ξ_2 are the excitation amplitude of clockwise and counterclockwise modes of the WGR-1. ξ_3 and ξ_4 are the excitation amplitudes of clockwise and counterclockwise modes of the WGR-2. Furthermore, the above amplitudes can be expressed formally as

$$\begin{aligned}
 \phi_{Ra}(x) &= e^{ikx} [\theta(-x) + t_{12}^a \theta(x) \theta(d-x) + t_a \theta(x-d)], \\
 \phi_{La}(x) &= e^{-ikx} [r_a \theta(-x) + r_{12}^a \theta(x) \theta(d-x)], \\
 \phi_{Rb}(x) &= e^{ikx} [t_{12}^b \theta(x) \theta(d-x) + t_b \theta(x-d)], \\
 \phi_{Lb}(x) &= e^{-ikx} [r_b \theta(-x) + r_{12}^b \theta(x) \theta(d-x)].
 \end{aligned} \tag{3}$$

where t_a and r_a are the transmission and reflection amplitudes in the waveguide- a , t_b and r_b are the transmission and reflection amplitudes in the waveguide- b , respectively. $\theta(x)$ is the

Heaviside step function with $\theta(0) = 1/2$. $t_{12}^{a(b)}\theta(x)\theta(d-x)$ and $r_{12}^{a(b)}\theta(x)\theta(d-x)$ represent the transferred amplitudes between the WGRs.

Solving the eigen-equation $H|\psi\rangle = E_k|\psi\rangle$, the expressions of t_a , r_a , t_b and r_b can be obtained as follows:

$$\begin{aligned}
t_a &= 1 + \frac{\Gamma_{1a}Q_2 + \Gamma_{2a}Q_1 - iB_a[u_1e^{i\phi(k)} + u_2]}{i[Q_1Q_2 + u_1u_2e^{i\phi(k)}]}, \\
r_a &= -\frac{iB_bS_1e^{i\phi(k)}[B_aQ_2 - iu_1\Gamma_{2a}e^{i\phi(k)}]}{i[Q_1Q_2 + u_1u_2e^{i\phi(k)}]} \\
&\quad + \frac{A_1S_2e^{i\phi(k)}(\Gamma_{2a}Q_1 - iB_a u_2)}{i[Q_1Q_2 + u_1u_2e^{i\phi(k)}]} \\
&\quad - \frac{iB_aS_2e^{i\phi(k)}(B_aQ_1 - iu_2\Gamma_{1a})}{i[Q_1Q_2 + u_1u_2e^{i\phi(k)}]} \\
&\quad + \frac{A_2S_1[\Gamma_{1a}Q_2 - iB_a u_1e^{i\phi(k)}]}{i[Q_1Q_2 + u_1u_2e^{i\phi(k)}]}, \\
t_b &= -\frac{iB_bS_1[Q_2D_1 - iu_1C_2e^{i\phi(k)}]}{i[Q_1Q_2 + u_1u_2e^{i\phi(k)}]} \\
&\quad + \frac{A_1S_2(Q_1C_2 - iu_2D_1)}{i[Q_1Q_2 + u_1u_2e^{i\phi(k)}]} \\
&\quad - \frac{iB_aS_2e^{i\phi(k)}(Q_1D_2 - iu_2C_1)}{i[Q_1Q_2 + u_1u_2e^{i\phi(k)}]} \\
&\quad + \frac{A_2S_1[Q_2C_1 - iu_1D_2e^{i\phi(k)}]}{i[Q_1Q_2 + u_1u_2e^{i\phi(k)}]}, \\
r_b &= \frac{Q_1C_2e^{i\phi(k)} + Q_2C_1 - ie^{i\phi(k)}(u_2D_1 + u_1D_2)}{i[Q_1Q_2 + u_1u_2e^{i\phi(k)}]}, \tag{4}
\end{aligned}$$

where $E_{kn} = E_k - (\omega_{cn} - i\gamma_{cn}/2)$, $\Gamma_{nm} = V_{nm}^2/v_g$, $A_n = E_{kn} + i(\Gamma_{na} + \Gamma_{nb})/2$, $B_m = \sqrt{\Gamma_{1m}\Gamma_{2m}}$, $C_n = \sqrt{\Gamma_{na}\Gamma_{nb}}$, $D_1 = \sqrt{\Gamma_{1a}\Gamma_{2b}}$, $D_2 = \sqrt{\Gamma_{2a}\Gamma_{1b}}$, $\phi(k) = 2kd$, $M = A_1A_2 + B_1B_2e^{i\phi(k)}$, $S_n = h_n/M$, $Q_1 = A_1 - A_2h_1S_1$, $Q_2 = A_2 - A_1h_2S_2$, $u_1 = B_2 + B_1h_1S_2$, and $u_2 = B_1 + B_2h_2S_1$.

Analytic expressions demonstrated above provide a complete description on the single-photon transport properties of the proposed network. Obviously, by properly designing the relevant geometric parameter d and the other physical parameters, such as the frequency of the incident photons, the waveguide-resonator coupling strengths V_{nm} , and the intermode interactions h_n , the desired photon routings can be implemented.

III. QUANTUM ROUTINGS OF SINGLE PHOTONS BY ENGINEERING THE WGRS

The quantum routing property of single photons is characterized by the transmission coefficient $T_{a(b)} = |t_{a(b)}|^2$ and reflection coefficient $R_{a(b)} = |r_{a(b)}|^2$. It is easily seen from Eq. (4) that these coefficients can be engineered.

A. Photonic routing with a single WGR

As a comparison, we first discuss the routing capability of a single WGR, by assuming $V_{2a} = V_{2b} = 0$. In Fig. 2, we plot $T_{a(b)}$ and $R_{a(b)}$ as a function of $\Delta\omega$ ($\Delta\omega = E_k - \omega_{c1}$) for different backscattering strengths without any dissipation. It is seen that

(i) For $h_1 = h = 0$, i.e., single bosonic routing case, one can see that $R_b = 1$ and $R_a = T_a = T_b = 0$ for $\Delta\omega = 0$. This indicates that, in the resonant case, the single photon is transferred completely into the left of the waveguide-b along with the sidewall of the resonator. In this case, the counter-clockwise mode of the WGR is not excited and thus the incident photon cannot transport to the left of waveguide-a and the right of waveguide-b.

(ii) With the intermode interaction between the bosonic modes in the GWR, i.e., $h_1 = h \neq 0$, R_a and T_b are out of zero. In this case, the photon is routed into four outputs, and the probabilities are allocated in four ports.

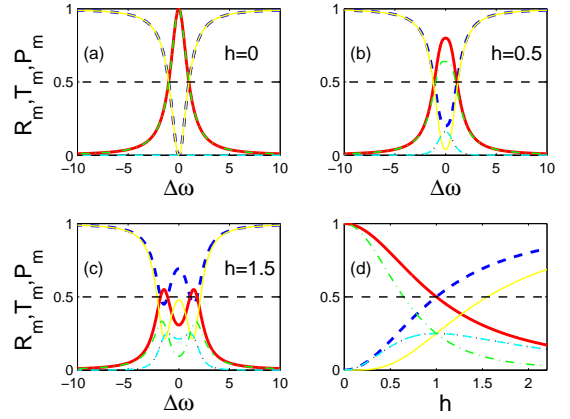


FIG. 2: (Color online) The transmission T_m (solid yellow T_a and dashed cyan T_b), reflection R_m (dotted black R_a and dash-dotted green R_b), and P_m (thick dashed blue P_a and thick solid red P_b) for different backscattering strengths (a) $h = 0$, (b) $h = 0.5$, (c) $h = 1.5$. (d) as a function of backscattering h for $\Delta\omega = 0.1$. Other parameters are $\gamma_1 = \gamma_2 = 0$, $\omega_c = 2\pi \times 6.0446\text{MHz}$ [21], $V_{1a} = V_{2a} = 1$. For convenience, all the parameters except the distance are in units of ω_c .

To specifically investigate how the backscattering strength h influence the routing between two channels, we plot P_a and P_b as a function $\Delta\omega$ for different backscattering strength h in Fig. 2, with $V_{1a} = V_{2a} = V_a = 1$. Here, $P_a = T_a + R_a$ and $P_b = T_b + R_b$ represent the probabilities of finding the incident single photons in the waveguide-a and the waveguide-b, respectively. Interesting, a large region of $P_b > 0.5$ in Fig. 2 (a) can emerge near the resonance point of the scattering spectra, in contrast to the usual single-emitter routing wherein $P_b \leq 0.5$ [9–12]. Physically, this may result from the special construction of the WGR, wherein the cyclic modes can couple and redirect the photons in waveguide-a into waveguide-b in the opposite direction, along with the sidewall of the resonator (see Fig. 1). Also, with the increase of the backscat-

tering strength h , R_b decreases rapidly and others increase to cross a dot with equal probabilities, and the region of $P_b > 0.5$ decreases gradually to zero around the point $h_1 = h = 1$, as shown in Fig. 2 (d). This may be due to the fact that, as increasing the backscattering strength, the counterclockwise propagation is favored and the transfer to waveguide-b is suppressed.

B. Photonic routings with double WGRs

Then we investigate the single-photon scattering properties in four ports in the double-resonator case. For simplicity, we assume that $\omega_{c1} = \omega_{c2} = \omega_c$, $h_1 = h_2 = h$, $V_{1a} = V_{2a} = V_a$, and $V_{1b} = V_{2b} = V_b$. We plot $T_{a(b)}$ and $R_{a(b)}$ as a function of $\Delta\omega$ ($\Delta\omega = E_k - \omega_c$) for different backscattering strengths under the distance $d = 2$ of two WGRs in Fig. 3. Similar to the single-resonator case, a large window of $P_b > 0.5$ appears near the resonance point, and the window decreases with the increase of the backscattering strength. Specifically, around the point $h = 2$, the probabilities allocated in the four ports meet at a equal-value dot, and P_b reduces to 0.5.

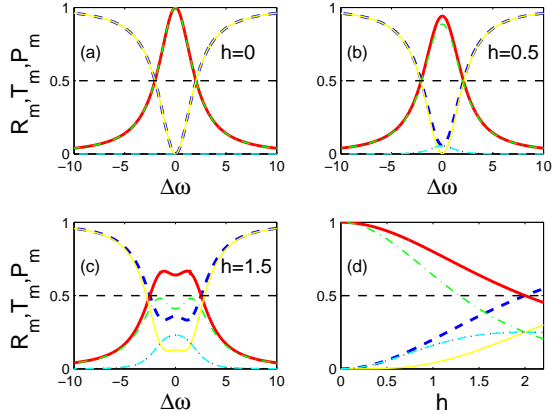


FIG. 3: (Color online) The transmission T_m (solid yellow T_a and dashed cyan T_b), reflection R_m (dotted black R_a and dash dotted green R_b), and P_m (thick dashed blue P_a and thick solid red P_b) for different backscattering strengths: (a) $h = 0$, (b) $h = 0.5$, (c) $h = 1.5$. (d) as a function of backscattering h for $\Delta\omega = 0$. Other parameters are $\gamma_1 = \gamma_2 = 0$, $V_a = V_b = 1$ and $d = 2$ (in unit of $1.6 \times 10^{-10} v_g/\omega_c$).

The coupling strengths between waveguides and WGRs also play a crucial role for the quantum routing property. We plot P_a and P_b as a function of the coupling strength $V = V_a = V_b$ under the non-resonance regime (e.g. $\Delta\omega = 0.42$) in Fig. 4. It is shown that, when the coupling strengths are shut down the incident single photon will transmit completely in the waveguide-a. When the coupling strengths are turned on, the probabilities of the single photon are allocated in two waveguides and a large region of high transfer appears as the incident single photon transfer from the waveguide-a to the waveguide-b.

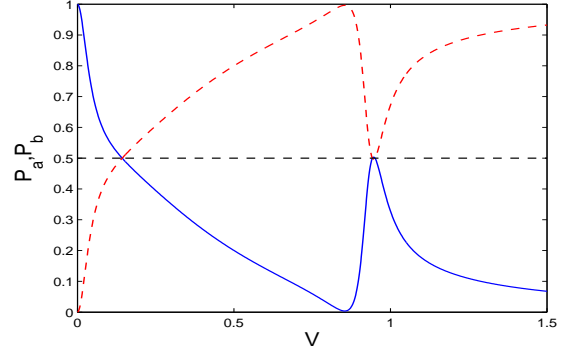


FIG. 4: (Color online) P_a (solid blue) and P_b (dashed red) as a function of waveguide-WGR coupling strength. These parameters are $\gamma_1 = \gamma_2 = 0$, $h = 0.5$, $\Delta\omega = 0.42$, $d = 1$ (in unit of $1.6 \times 10^{-9} v_g/\omega_c$).

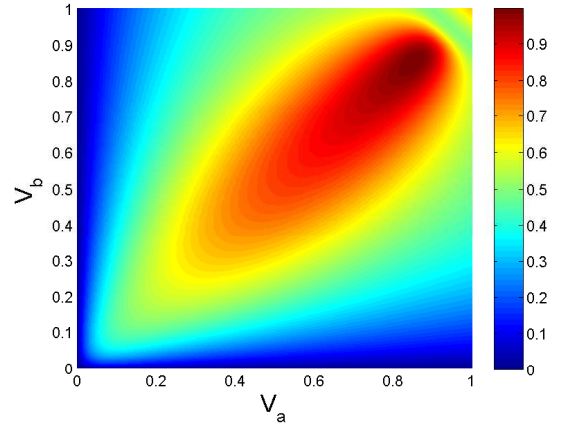


FIG. 5: (Color online) P_b as functions of waveguide-WGR coupling strengths V_a and V_b . These parameters are the same as Fig. 4.

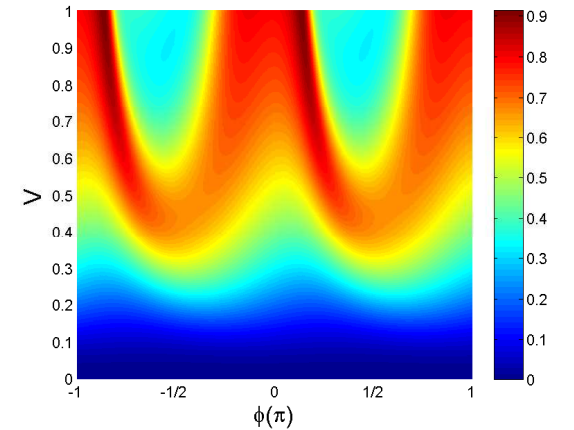


FIG. 6: (Color online) P_b as functions of phase shift $\phi(k)$ and coupling strength V . These parameters are $\gamma_1 = \gamma_2 = 0$, $h = 1$, $\Delta\omega = 0.42$.

To gain a deeper insight into the dependence of the inter-channel transport on the waveguide-WGR couplings, Fig. 5 displays the transfer rate P_b versus the different couplings of two waveguides. It is seen that, when V_a and V_b are both small the incident photon cannot be redirected from the waveguide-a into the waveguide-b completely. Increasing the couplings, a large window of high transfer rate emerges. More interestingly, the transfer rate P_b can reach a maximum value $P_b = 0.996 \approx 1$ at the equal value location around $V_a = V_b = 0.85$, which means that the perfect transfer can almost be realized.

Fig. 6 shows specifically how the transfer rate P_b against the coupling strength and phase shift ϕ for the typical parameters $h = 1$ and $\Delta\omega = 0.42$. As seen, with increasing the coupling strength a wide region of $P_b > 0.5$ appears, and even high transfer rates of $P_b > 0.9$ are located in the region. It is also found that the transfer rate of P_b is a periodic function of the phase shift, and two small regions with low transfer rate ($P_b < 0.5$) emerge near the standing wave antinodes with $\phi = \pm\pi/2$.

C. Engineering the Fano-like resonances

Fano resonances are the popular resonant scattering phenomena of the electric and magnetic transports in many condensed matter systems. Due to the interference between the photonic waves, the Fano-like resonance may also appear. To investigate such a phenomenon, we examine the routing property of the single photon from the input quantum channel to another one. Fig. 7 displays P_a and P_b as a function $\Delta\omega$ for the different distance d of the two WGRs, with $V_a = V_b = 1$ and $h = 0.5$. Obviously, for $d = 0$ the system reduces to the single-resonator case without any interference of the photonic wave. As a consequence, the Fano-like resonance doesn't emerge. With the increase of d , the jiggling behavior emerges due to multiple interference of waves, and the feature of Fano-like resonance becomes more evidently. Physically, the WGR-1 (WGR-2) is served as a delocalized (localized) channel for the single photon passing through it, and thus the interference between these two channels results in the asymmetric line shape [32–34]. Certainly, increasing the distance of two WGRs enhances the interference between the two channels, and thus leads to more distinct Fano-line shapes.

IV. CONCLUSIONS AND DISCUSSIONS

Certainly, in the real experiments the dissipation of WGR is inevitable during propagation, although it is significantly weaker than the usual atom and single-mode resonator. Specifically, we plot the transfer rate P_a , P_b and loss L ($L = 1 - P_a - P_b$) for certain dissipations in Fig. 8, with $h = 0.5$ and $d = 1$. It is seen that the altitude of P_b decreases slightly with the increase of dissipation. Therefore, the proposed double-WRG quantum router should be robust for the further possible applications.

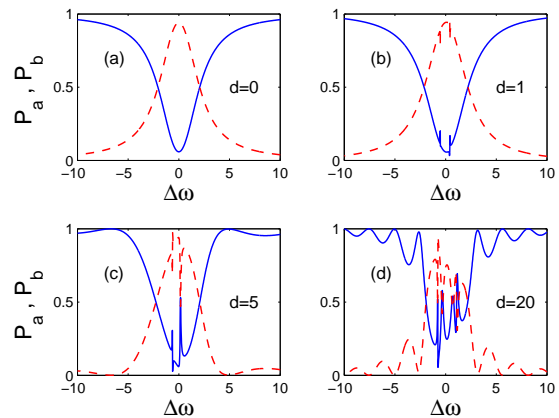


FIG. 7: (Color online) P_a (solid blue) and P_b (dashed red) for different distance of the two WGRs (a) $d = 0$, (b) $d = 1$, (c) $d = 5$ and (d) $d = 20$ (in unit of $1.6 \times 10^{-9} v_g / \omega_c$), respectively. Other parameters are $\gamma_1 = \gamma_2 = 0$, $V_a = V_b = 1$ and $h = 0.5$.

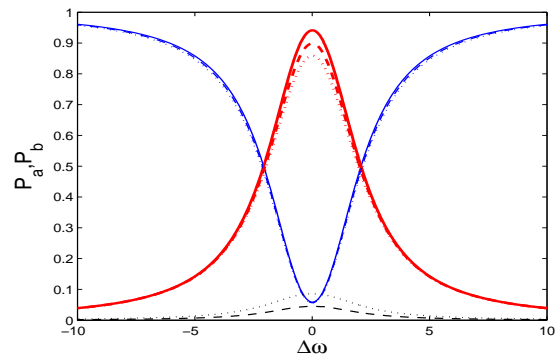


FIG. 8: (Color online) P_a (blue line), P_b (red line) and loss L ($L = 1 - P_a - P_b$) (black line at the bottom of the plot) versus $\Delta\omega$ for different dissipation in the WGRs $\gamma_c = 0$ (solid line), $\gamma_c = 0.1$ (dashed line) and $\gamma_c = 0.2$ (dotted line). Other parameters are $h = 0.5$, $V_a = V_b = 1$ and $d = 1$ (in unit of $1.6 \times 10^{-9} v_g / \omega_c$).

In summary, we have investigated the single-photon quantum routing produced by a double-WRG quantum router. Using a full quantum theory, the single-photon transmission and reflection amplitudes were analytically obtained. By numerical method, we analyzed the relevant transport properties in detail. It is found that, by properly setting the relevant parameters, single-photon scattering into four ports can be designed conveniently. Moreover, Fano-like resonance, due to the quantum interference, is exhibited in the scattering spectra. Our results showed that high routing capability from input channel to another channel can be achieved near resonance by only a single resonator, also implemented by adjusting the distance of two WGRs and the coupling strengths between waveguide and WGR, even in the nonresonance regime. Therefore, the proposed system could be utilized as a robust quantum router.

Acknowledgments

This work was supported by the National Natural Science Foundation of China (Grant Nos. 11247032 and U1330201)

and the Natural Science Foundation of Jiangxi (Grant No. 20151BAB202012).

-
- [1] H. J. Kimble, *Nature (London)* **453**, 1023 (2008).
- [2] T. Aoki, A. S. Parkins, D. J. Alton, C. A. Regal, Barak Dayan, E. Ostby, K. J. Vahala, and H. J. Kimble, *Phys. Rev. Lett.* **102**, 083601 (2009).
- [3] I.-C. Hoi, C. M. Wilson, G. Johansson, T. Palomaki, B. Peropadre, and P. Delsing, *Phys. Rev. Lett.* **107**, 073601 (2011).
- [4] J.-T. Shen and S. Fan, *Opt. Lett.* **30**, 2001 (2005).
- [5] J.-T. Shen and S. Fan, *Phys. Rev. Lett.* **95**, 213001 (2005).
- [6] D. E. Chang, A. S. Sørensen, E. A. Demler, and M. D. Lukin, *Nat. Phys.* **3**, 807 (2007).
- [7] L. Zhou, Z. R. Gong, Yu-xi Liu, C. P. Sun, and F. Nori, *Phys. Rev. Lett.* **101**, 100501 (2008).
- [8] J.T. Shen, S. Fan, *Phys. Rev. A* **79** 023837 (2009).
- [9] L. Zhou, L. P. Yang, Y. Li, and C. P. Sun, *Phys. Rev. Lett.* **111**, 103604 (2013).
- [10] J. Lu, L. Zhou, L. M. Kuang, and F. Nori, *Phys. Rev. A* **89**, 013805 (2014).
- [11] W. B. Yan, B. Liu, L. Zhou, and H. Fan, *Europhys. Lett.* **111**, 64005 (2015).
- [12] J. Lu, Z. H. Wang, and L. Zhou, *Opt. Express* **23**, 22955(2015).
- [13] G. S. Agarwal and S. Huang, *Phys. Rev. A* **85**, 021801 (2012).
- [14] K. Xia and J. Twamley, *Phys. Rev. X* **3**, 031013 (2013).
- [15] K. Lemr, K. Bartkiewicz, A. Černoč, and J. Soubusta, *Phys. Rev. A* **87**, 062333 (2013).
- [16] X. S. Ma, S. Zotter, J. Kofler, T. Jennewein, and A. Zeilinger, *Phys. Rev. A* **83**, 043814 (2011).
- [17] I. Shomroni, S. Rosenblum, Y. Lovsky, O. Brechler, G. Guendelman, and B. Dayan, *Science* **345**, 903(2014).
- [18] Xingmin Li and L. F. Wei, *Phys. Rev. A* **92**, 063836 (2015); Xingmin Li, Lingyun Xie, and L. F. Wei, *Phys. Rev. A* **92**, 063840(2015).
- [19] K. Nozaki, T. Tanabe, A. Shinya, S. Matsuo, T. Sato, H. Taniyama, and M. Notomi, *Nat. Photonics* **4**, 477 (2010).
- [20] A. Poon, X. Luo, F. Xu, and H. Chen, *Proc. IEEE* **97**, 1216 (2009).
- [21] J. T. Shen, S. Fan, *Phys. Rev. A* **79** 023838 (2009).
- [22] Sandra Isabelle Schmid and Jörg Evers, *Phys. Rev. A* **84** 053822 (2011).
- [23] F.-Y. Hong and S.-J. Xiong, *Phys. Rev. A* **78**, 013812 (2008).
- [24] F.-Y. Hong and S.-J. Xiong, *Nanoscale Res. Lett.* **3**, 361 (2008).
- [25] W. Yao, R.-B. Liu, and L. J. Sham, *Phys. Rev. Lett.* **95**, 030504 (2005).
- [26] H. Ajiki and H. Ishihara, *Phys. Status Solidi* **3**, 2440 (2006).
- [27] A. H. Safavi-Naeini, T. P. M. Alegre, J. Chan, M. Eichenfield, M. Winger, Q. Lin, J. T. Hill, D. E. Chang, and O. Painter, *Nature (London)* **472**, 69 (2011).
- [28] S. Groeblacher, K. Hammerer, M. R. Vanner, and M. Aspelmeyer, *Nature (London)* **460**, 724 (2009).
- [29] A. D. O’Connell, M. Hofheinz, M. Ansmann, R. C. Bialczak, M. Lenander, E. Lucero, M. Neeley, D. Sank, H. Wang, M. Weides, J. Wenner, J. M. Martinis, and A. N. Cleland, *Nature (London)* **464**, 697 (2010).
- [30] S. Weis, R. Riviere, S. Deleglise, E. Gavartin, O. Arcizet, A. Schliesser, and T. J. Kippenberg, *Science* **330**, 1520 (2010).
- [31] T. Rocheleau, T. Ndukum, C. Macklin, J. B. Hertzberg, A. A. Clerk, and K. C. Schwab, *Nature (London)* **463**, 72 (2010).
- [32] W. Chen, G. Y. Chen, and Y. N. Chen, *Opt. Lett.* **18**, 10360 (2010).
- [33] G. Y. Chen, Y. N. Chen, *Opt. Lett.* **37**, 4023 (2012).
- [34] G. Y. Chen, M. H. Liu, Y. N. Chen, *Phys. Rev. A* **89**, 053802 (2014).